

Image Quality and Change of Illuminant: An Information-Theoretic Evaluation

Steven Le Moan, Philipp Urban

Institute of Printing Science and Technology, Technische Universität Darmstadt, Germany

Abstract

We investigate the influence of scene illuminant on perceived image quality. Given two multispectral images, an original and a reproduction (e.g. compressed, gamut mapped,...), we seek redundancies of perceived difference through changes of illuminant, and with regard to 5 so-called image difference features (IDF). In order to do this, we employ an information-theoretic perspective to measure variations of entropies in each IDF, w.r.t. various scene illuminants, and in the case of two particular kinds of distortions: spectral gamut mapping and a spectral reconstruction from a six-channel camera model. Our results indicate that changing the scene illuminant has a lesser influence on achromatic image difference features.

Introduction

Most recent studies on Image Quality Assessment (IQA) rely on greyscale [1, 2] or chromatic information [3] to rate the difference between two images. The intent is to correlate as much as possible with human's judgment under specific viewing conditions. Yet, with the advent of spectral technologies, image appearance models and multi-channel printing, there is a growing need for a higher dimensional IQA. Spectral acquisition, processing and reproduction methods (e.g. spectral gamut mapping [4, 5], spectral separation [6], compression [7], dimensionality reduction [8, 9]), require a new range of measures for Spectral Image Quality Assessment (SIQA).

Although criteria such as classification or target detection accuracy are widely used for spectral quality in remote sensing applications, very little work has actually been done to evaluate spectral quality in terms of perception. In [10], [11] and [12], various spectral-based distances and divergence measures were studied for hyper- and multi-spectral image quality, with attempts to relate these quantities to perceptual meanings. Although they might correlate with human judgment in some cases, measures that operate directly in spectral space such as the popular Root-Mean Square Error or the Goodness-of-Fit Coefficient, are usually unable to properly do so. A reasonable explanation to this is that the very notion of color (at least in terms of perception) exists only when Viewing Conditions (VC) are specified. Without considering at least a scene illuminant and an observer model, no assumptions can be made on how reflectance spectra are interpreted by the human visual system. An alternative strategy is to pool the scores from a traditional image difference measures like CIE2000 over a variety of VC [13], but to which extent? How much,

and which aspects of the perceptual difference between two images remain unchanged from one set of VC to another (e.g. from daylight to incandescent light)?

In this study, we investigate such questions, in order to better understand the key challenges in SIQA. We propose to use a set of 5 image-difference features introduced by Lissner *et al.* [3], and to observe their behavior when the scene illuminant changes. In order to do this, we employ an information-theoretic perspective [2, 14] to measure variations of entropies in each feature, w.r.t. various scene illuminants, and in the case of two particular kinds of distortions: spectral gamut mapping and spectral reconstruction from a six-channel camera model. Note that the most influential VC feature is certainly the spectral power distribution of the scene illuminant. Therefore, this study focuses solely on changes of illuminant, while the remaining VC (e.g. standard observer) are assumed to be constant.

Image difference features

In order to better understand how image differences are changed with the scene illuminant, we rely on the Image-Difference Features (IDF) used for the Color Image-Difference (CID) measure [3]. In the CID framework, the two images to compare are first normalized with an image-appearance model, including a CAT02 chromatic adaptation (as used by CIECAM02). This is to take into account "the human visual system's capability to adjust to widely varying colors of illumination in order to approximately preserve the appearance of object colors" [16]. The images are then converted into the nearly perceptually uniform LAB2000HL color space [17]. IDF maps are then computed by means of terms adapted from the SSIM index [1] within sliding windows (see formulas in Appendix). Five maps are therefore obtained: Lightness-Difference map (\mathbf{L}_L), Lightness-Contrast map (\mathbf{C}_L), Lightness-Structure map (\mathbf{S}_L), Chroma-Difference map (\mathbf{L}_C) and Hue-Difference map (\mathbf{L}_H). Figure 1 illustrates the workflow from spectral space to feature extraction. We refer to the original paper [3] and the source code provided by Lissner *et al.* [18] for further explanations about the measure.

Note that the CID measure compares tri-chromatic images, therefore each IDF map is intrinsically linked to certain viewing conditions. The conversion from reflectance data to CIEXYZ tristimuli, was made w.r.t. a CIE 2° standard observer, and a variety of illuminants. In a previous, recent work [15], we observed that CID scores computed for a few illuminants are able to predict image difference under a large variety. In this study, we aim to

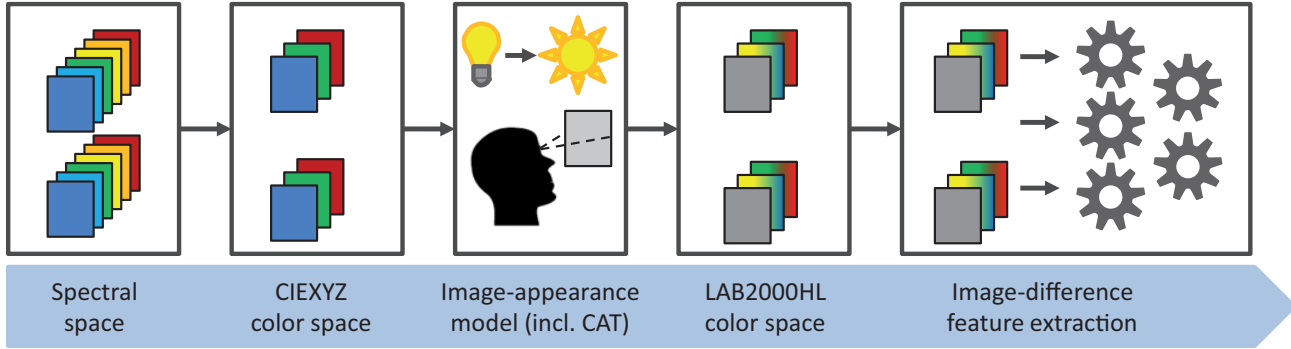


Figure 1. Part of the CID workflow, from spectral space to feature extraction. The figure is partially extracted from [15].

quantify and better understand the variability of each IDF.

Redundancies

Given the IDF maps under a variety of illuminants, we wish to evaluate their respective content in terms of information. Measures based on Shannon’s entropy [19] provide an efficient probabilistic framework to do so. Moreover, when applied to data with perceptual attributes, they ensure that the abstract notion of information relates to a perceptual quantity. The entropy of an IDF map is a measure of its uncertainty. It is usually measured in *bits*, that is the number of bits required to code the full map. The more bits are required to code all the coefficients of the map, the more information it contains. We denote $H(X)$ the entropy of the discrete random variable X , which is estimated as follows:

$$H(X) = - \sum_{x=0}^N p_x \log_2(p_x) \quad (1)$$

where $\{0 \dots N\}$ is the range of the sample data (in the case our 8-bit IDF maps, $N = 255$) and p_x is the probability density function of X (the probability that X takes the value x), usually estimated by the data’s histogram. Note that the use of base 2 for the logarithm is the reason why the unit of $H(X)$ is the *bit*.

Figures 2a and 2b illustrate the interaction of a pair of spectral images and their respective renderings, in terms of information. The sought-after quantity in this study is the red zone in Figure 2b, a complex overlap of information between several variables, depicting the difference between the two images that is common to all illuminants. Not only do we aim to quantify it, we also wish to understand what it is made of, to evaluate which IDFs are the least and most sensitive to illuminant changes. Measures based on joint entropies, such as the conditional co-information [20] could be very practical for these tasks. The joint entropy of a couple of variables depict how much information they engender, as a couple. Unfortunately, the estimation of joint probability density functions is burdened by the curse of dimensionality [21], which implies that the number of samples needed for an accurate estimation grows almost

exponentially with the number of variables. Relying on the graph of Figure 2, this means that the more ellipses are overlapping, the more difficult it is to measure their overlap. Consequently, the influence of no more than 4 or 5 illuminants could be evaluated for a megapixel image.

Another approach is to assess the extent to which the effect of variations of illuminant can be detected with a limited number of degrees of freedom. That is, how much of the image difference is gained through these variations, given a representative, meaningful and low-dimensional reference (see Figure 2c). Let us denote Θ the set of illuminants under consideration and \mathbf{L}_L^Υ , \mathbf{C}_L^Υ , \mathbf{S}_L^Υ , \mathbf{L}_C^Υ , \mathbf{L}_H^Υ the set of IDF maps obtained when the two spectral images to compare are rendered with illuminant Υ . We propose to use the first Principal Components (PCs) of Θ to create a small number of reference (so-called *synthetic*) illuminants, that we will denote by PC_1, PC_2, \dots . Consequently, we aim to measure the average gain of information of $\mathbf{L}_L^\Upsilon, \forall \Upsilon \in \Theta$, given $\mathbf{L}_L^{PC_1}$, and respectively for the other IDFs. This gain can be measured by the conditional entropy, defined as follows:

$$H(X|Y) = - \sum_{x=0}^N \sum_{y=0}^N p_{x,y} \log_2 \frac{p_{x,y}}{p_y} \quad (2)$$

where $p_{x,y}$ is the joint density function of X and Y , computed by their joint histogram.

On this basis, $H(\mathbf{L}_L^{D65} | \mathbf{L}_L^{PC_1})$ denotes the gain of Lightness-Difference information for a D65 rendering and $H_{L_L}^{PC_1}$ refers to the average over all illuminants in Θ . Note that we also allow the reference to be multi-dimensional, that is to measure the gain given not one but several PCs, such as $H(\mathbf{L}_L^{D65} | \mathbf{L}_L^{PC_1}, \mathbf{L}_L^{PC_2})$. The greater the dimensionality of the entropy, the greater the number of samples required for a reasonable accuracy. Therefore, we consider only the two first PCs of Θ in this study.

If the average gain of IDF information is low, it means that only a few PCs are sufficient to accurately predict the perceptual image difference under any illuminant. Figure 3 shows an example.

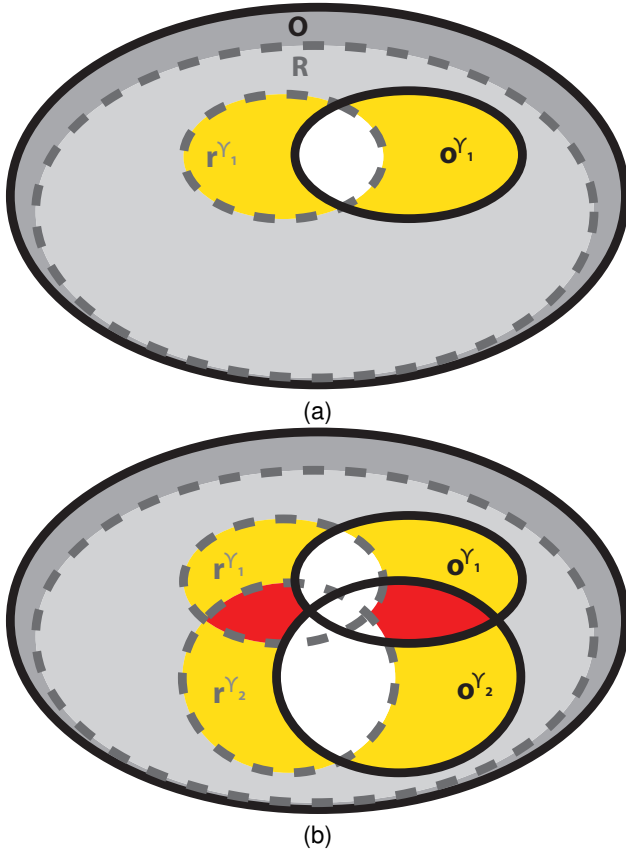


Figure 2. Diagram representation of information interactions. Each ellipse represents the information spanned by an image. The two largest ellipses, noted \mathbf{O} and \mathbf{R} (solid and dashed line) represent an original spectral image and a given reproduction (respectively). Note that it is likely (but not necessary) that a reproduction contains less information than the original. In (a), the smaller ellipses describe the renderings \mathbf{o}^{Υ_1} and \mathbf{r}^{Υ_1} , under illuminant Υ_1 . The grayed areas therefore represent the information that is discarded by the human visual system, e.g. the identification of parameric pairs [14]. The white area represent the overlap of information between both renderings (mutual information), whereas the yellow parts depict the information that exist in one rendering but not the other, i.e. the image difference. In (b), a second illuminant is considered: Υ_2 . The red areas depict the overlap of perceived image difference, that is for example the artifacts that are equally annoying under both illuminants.

Experiments and Results

Illuminants

For our experiments, we used a total of 74 illuminants in Θ : four CIE daylights (D50, D65, D80 and D100), the CIE A and Fluorescent Series as well as the full collection made available by the National Gallery of London [22], which includes LED, fluorescent and tungsten-based lights. For the sake of clarity, Figure 4 depicts only the three first PCs extracted from this set. All illuminants were normalized to the intensity range $[0, 1]$, including the synthetic ones (given that principal component analysis may produce negative values).

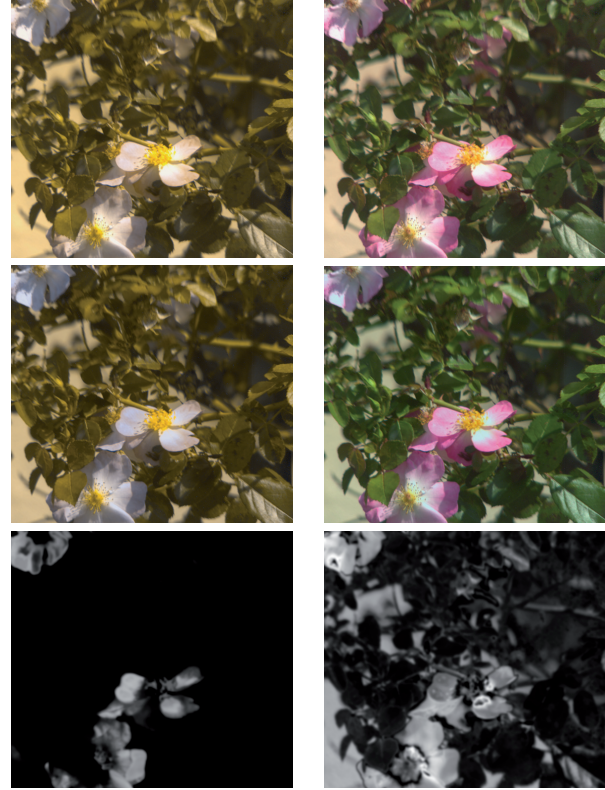


Figure 3. Examples of \mathbf{L}_H maps under PC1 (left column) and D65 (right column). The first row corresponds to the original image, while the second row depicts the camera model-based reproduction ($\mathbf{R3}$). The conditional entropy value is $H(\mathbf{L}_H^{D65} | \mathbf{L}_H^{PC1}) = 5.4$ bits, which is relatively high provided that these maps are coded on 8 bits (256 levels). This means that, in order to predict hue discrepancies under D65, the first PC of Θ is not a sufficient reference.

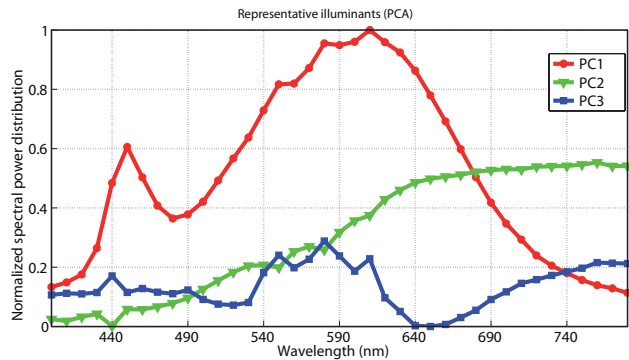


Figure 4. Representative, so-called "synthetic", illuminants. PC1 and PC2 respectively contain 59.8 and 88.5% of the energy in Θ .

Images

The 8 multispectral images of natural scenes from Foster's 2002 database [23] were used in this study. They contain 31 channels covering the visible wavelengths range.

To create distorted images, we rendered reproductions for each reference image based on three kinds of distortions:



Figure 5. Examples of renderings under D65 illuminant. Column-wise: original, **R1**, **R2** and **R3**.

- **Spectral gamut mapping 1:** We considered the spectral gamut of a Canon iPF5000 printer utilizing CMYKRGB inks, and a naive approach that uses CIELAB and D65 illuminant to map the out-of-gamut pixels to their closest in-gamut pixels, w.r.t. ΔE_{ab}^* . From the resulting CIELAB pixels, printable metamers were selected randomly, yielding a spectral in-gamut image, denoted by **R1**.
- **Spectral gamut mapping 2:** With the same gamut, we applied the method presented in [5]. We used D65 and A as principal and secondary illuminants, respectively. The resulting spectral reproduction is denoted by **R2**.
- **Spectral camera model:** We simulated how a customized 6-channel Sinar camera with known spectral sensitivity functions would acquire the scenes. Reflectance curves were then reconstructed by means of the pseudo-inverse method (see for instance [24]), using a reduced set of Macbeth ColorChecker spectra [25]. No noise nor point spread functions were considered in the model. The resulting spectral reproduction is denoted by **R3**.

Figure 5 gives an example of renderings under D65. The conversion from reflectance data to CIEXYZ tristimuli was made w.r.t. a CIE 2° standard observer. As previously explained, we assume that changing the illuminant has a far greater influence on the rendering than a change of observer.

Results

Figures 6, 7 and 8 show the results obtained. Note that over the 8 images of the database, we observed relatively small standard deviations overall. This shows a limited influence of the scene on these results.

We note that the three reproductions yield different trends, obviously depending on their relative characteristics. The naive gamut mapping engenders the worst predictability in terms of contrast and structure, which is in accordance to the fact that it does not consider any spatial information. On the other hand, the second gamut mapping presents a very good stability in terms of lightness-bases features. Not only do different kinds of distortion affect different IDF's, they also affect how these IDF's vary under different illuminants. Even considering a same gamut, two spectral gamut mapping approaches can render im-

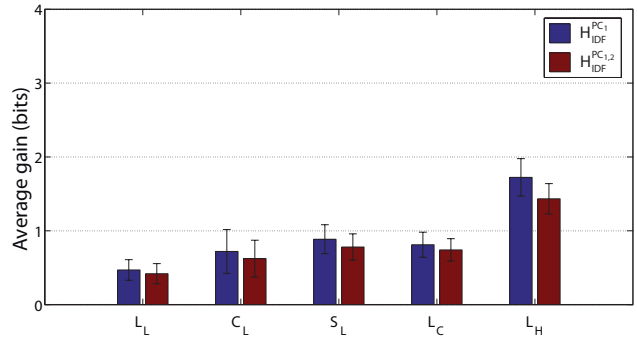


Figure 6. Average conditional entropies H_{IDF}^{PC1} and $H_{IDF}^{PC1,PC2}$ on 8 gamut-mapped images (**R1**).

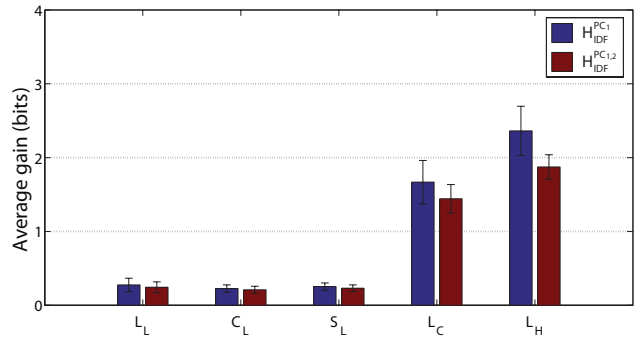


Figure 7. Average conditional entropies H_{IDF}^{PC1} and $H_{IDF}^{PC1,PC2}$ on 8 gamut-mapped images (**R2**).

ages that react in drastically different ways to illuminant changes. It seems however that these graphs have a few common trends. For instance, the least predictable attributes are always the chroma and hue, and particularly the latter. These chromatic IDF's also engender the largest drops between $H_{L_H}^{PC1}$ and $H_{L_H}^{PC1,2}$, as well as the largest standard deviations across our experimental data, especially in the case of **R3**. Otherwise, the C_L is overall the best predictable IDF.

In the end, when considering a large variety of illumi-

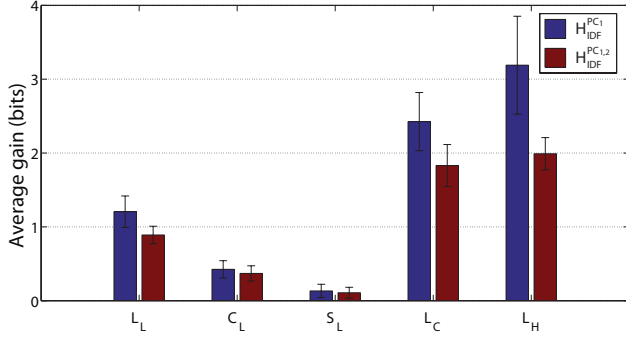


Figure 8. Average conditional entropies H_{IDF}^{PC1} and $H_{IDF}^{PC1,PC2}$ on 8 images distorted by means of a 6-channel multispectral camera model (R3).

nants, although one representative can be enough to predict variations of achromatic differences, chroma and hue discrepancies are more critical and thus require more information to be predicted with a sufficient accuracy.

Conclusion

We investigated the influence of scene illuminant on perceived image quality, from the perspective of information theory. Given two multispectral images, an original and a reproduction (compressed, gamut mapped,...), we observed interesting trends in terms of redundancies of perceived difference through changes of illuminant, with regard to 5 so-called image difference features. We showed that not only do different kinds of distortion affect different quality features, they also affect how these features vary under different illuminants. Particularly, our preliminary results indicate that changing the scene illuminant has a lesser influence on achromatic image difference features. Consequently, spectral reproduction methods such as spectral gamut mapping or spectral reconstruction need not to consider these as much as chroma and hue preservation across illuminants. This conclusion creates new perspectives for instance for the design of a low-dimensional Profile Connection Space allowing to compare spectral image with a limited number of features.

Acknowledgments

This work was supported by the Marie Curie Initial Training Networks (ITN) CP7.0 N-290154 funding.

Appendix: Image Difference Features

The following equations describe the 5 IDF's used in [3] and investigated in this study. As previously explained, these terms are derived from the SSIM index. They are computed within sliding windows \mathbf{x} and \mathbf{y} in the compared images X and Y (resp.). Each pixel x consists of a lightness and two chromatic values: $x = (L_x, a_x, b_x)$. The chroma of the pixel is defined as $C_x = \sqrt{a_x^2 + b_x^2}$. Note that the LAB2000HL colorspace [17] is used in this study for it has improved properties regarding perceptual uniformity and hue linearity compared to CIELAB.

1. Lightness, chroma, and hue comparisons:

$$l_L(\mathbf{x}, \mathbf{y}) = \frac{1}{c_1 \cdot \overline{\Delta L(\mathbf{x}, \mathbf{y})}^2 + 1}, \quad (3)$$

$$l_C(\mathbf{x}, \mathbf{y}) = \frac{1}{c_4 \cdot \overline{\Delta C(\mathbf{x}, \mathbf{y})}^2 + 1}, \quad (4)$$

$$l_H(\mathbf{x}, \mathbf{y}) = \frac{1}{c_5 \cdot \overline{\Delta H(\mathbf{x}, \mathbf{y})}^2 + 1}, \quad (5)$$

where $\overline{\Delta L(\mathbf{x}, \mathbf{y})}$, $\overline{\Delta C(\mathbf{x}, \mathbf{y})}$ and $\overline{\Delta H(\mathbf{x}, \mathbf{y})}$ denote the Gaussian-weighted mean of pixel-wise Lightness, Chroma and Euclidean Hue differences computed for each pixel pair (x, y) in the window.

2. Lightness-contrast comparison, according to [1]:

$$c_L(\mathbf{x}, \mathbf{y}) = \frac{2\sigma_x\sigma_y + c_2}{\sigma_x^2 + \sigma_y^2 + c_2}, \quad (6)$$

where σ_x and σ_y are the standard deviations in the lightness component of the sliding windows.

3. Lightness-structure comparison, according to [1]:

$$s_L(\mathbf{x}, \mathbf{y}) = \frac{\sigma_{\mathbf{xy}} + c_3}{\sigma_x\sigma_y + c_3}, \quad (7)$$

where $\sigma_{\mathbf{xy}}$ corresponds to the cosine of the angle between $\mathbf{x} - \bar{\mathbf{x}}$ and $\mathbf{y} - \bar{\mathbf{y}}$ [1] in the lightness component.

The following values were used for the IDF parameters: $c_1 = c_4 = 0.002$, $c_2 = c_3 = 10$, $c_5 = 0.02$.

References

- [1] Z. Wang, A.C. Bovik, H.R. Sheikh, and E.P. Simoncelli, "Image quality assessment: From error visibility to structural similarity," *IEEE Transactions on Image Processing*, vol. 13, no. 4, pp. 600–612, 2004.
- [2] H.R. Sheikh and A.C. Bovik, "Image information and visual quality," *IEEE Transactions on Image Processing*, vol. 15, no. 2, pp. 430–444, 2006.
- [3] I. Lissner, J. Preiss, P. Urban, M. Scheller Lichtenauer, and P. Zolliker, "Image-difference prediction: From grayscale to color," *IEEE Transactions on Image Processing*, vol. 22, no. 2, pp. 435–446, 2013.
- [4] S. Tsutsumi, M. R. Rosen, and R. S. Berns, "Spectral Gamut Mapping using LabPQR," *Journal of Imaging Science and Technology*, vol. 51, no. 6, pp. 473–485, 2007.
- [5] P. Urban and R. S. Berns, "Paramer Mismatch-based Spectral Gamut Mapping," *IEEE Transactions on Image Processing*, vol. 20, no. 6, pp. 1599–1610, 2011.
- [6] P. Urban, M. R. Rosen, and R. S. Berns, "Fast Spectral-Based Separation of Multispectral Images," in *IS&T/SID, 15th Color Imaging Conference*, Albuquerque, New Mexico, 2007, pp. 178–183.
- [7] S. Yu, Y. Murakami, T. Obi, M. Yamaguchi, and N. Ohyama, "Multispectral image compression for improvement of colorimetric and spectral reproducibility by nonlinear spectral transform," *Optical review*, vol. 13, no. 5, pp. 346–356, 2006.

- [8] J.S. Tyo, A. Konsolakis, D.I. Diersen, and R.C. Olsen, "Principal-components-based display strategy for spectral imagery," *IEEE Transactions on Geoscience and Remote Sensing*, vol. 41, no. 3, pp. 708–718, 2003.
- [9] N.P. Jacobson and M.R. Gupta, "Design goals and solutions for display of hyperspectral images," *IEEE Transactions on Geoscience and Remote Sensing*, vol. 43, no. 11, pp. 2684–2692, 2005.
- [10] E. Christophe, D. Léger, and C. Mailhes, "Quality criteria benchmark for hyperspectral imagery," *IEEE Transactions on Geoscience and Remote Sensing*, vol. 43, no. 9, pp. 2103–2114, 2005.
- [11] F.H. Imai, M.R. Rosen, and R.S. Berns, "Comparative study of metrics for spectral match quality," in *Proceedings of the First European Conference on Colour in Graphics, Imaging and Vision*, 2002, pp. 492–496.
- [12] JAS Viggiano, "Metrics for evaluating spectral matches: a quantitative comparison," in *Proceedings of the 2nd European Conference on Colour Graphics, Imaging and Vision*, 2004, pp. 286–291.
- [13] P. Morovič, J. Morovič, J. Arnabat, and J. García-Reyero, "Revisiting spectral printing: A data driven approach," in *Proceedings of the 20th Color Imaging Conference*. 2012, pp. 335–340, IS&T.
- [14] David H Foster, Iván Marín-Franch, Kinjiro Amano, and Sérgio Nascimento, "Approaching ideal observer efficiency in using color to retrieve information from natural scenes," *JOSA A*, vol. 26, no. 11, pp. B14–B24, 2009.
- [15] S. Le Moan and P. Urban, "Evaluating the perceived quality of spectral images," in *(to be published) Image Processing, 20th International Conference on*. September 2013, IEEE.
- [16] M.D. Fairchild, *Color appearance models*, J. Wiley, 2005.
- [17] I. Lissner and P. Urban, "Toward a unified color space for perception-based image processing," *IEEE Transactions on Image Processing*, vol. 21, no. 3, pp. 1153–1168, 2012.
- [18] "Supplementary material (Color image difference (CID) measure) available at: <http://www.idd.tu-darmstadt.de/color/papers> (2012/08/14)," .
- [19] C.E. Shannon and W. Weaver, "A mathematical theory of communication," *The Bell System Technical Journal*, vol. 27, pp. 379–423, 1948.
- [20] A.J. Bell, "The co-information lattice," in *Proceedings of the Fifth International Workshop on Independent Component Analysis and Blind Signal Separation*, 2003.
- [21] Dan Stowell and Mark D Plumbley, "Fast multidimensional entropy estimation by k-d partitioning," *Signal Processing Letters, IEEE*, vol. 16, no. 6, pp. 537–540, 2009.
- [22] "Spectral power distribution curves, the national gallery: <http://research.ng-london.org.uk/scientific/spd/>," last check: August 16, 2013.
- [23] S.M.C. Nascimento, F.P. Ferreira, and D.H. Foster, "Statistics of spatial cone-excitation ratios in natural scenes," *Journal of the Optical Society of America A*, vol. 19, no. 8, pp. 1484–1490, 2002.
- [24] J.Y. Hardeberg, F. Schmitt, H. Brettel, J.P. Crettez, and H. Maitre, "Multispectral image acquisition and simulation of illuminant changes," *Colour imaging: vision and technology*, pp. 145–164, 1999.
- [25] Steven Hordley, Graham Ffinalyson, and Peter Morovic, "A multi-spectral image database and its application to image rendering across illumination," in *Image and Graphics, 2004. Proceedings. Third International Conference on*. IEEE, 2004, pp. 394–397.